

Electronic Supplementary information: Quantitative photoacoustic spectral transformations in theranostic Solid Lipid Nanoparticles labelled with increasing concentrations of a Photoacoustic NIR BODIPY

Clément Linger,^{a,b} Giulia Maccini,^a Gilles Clavier,^c Rachel Méallet,^d Nicolas Tsapis,^{‡*a} and Jérôme Gateau ^{‡*b}

^a Institut Galien Paris-Saclay (IGPS), Université Paris-Saclay, CNRS, 91400 Orsay, France.

^b Laboratoire d'Imagerie Biomédicale (LIB), Sorbonne Université, CNRS, Inserm, 75006 Paris, France.

^c Photophysique et Photochimie Supramoléculaires et Macromoléculaires (PPSM), ENS Paris-Saclay, Université Paris-Saclay, CNRS, 91190, Gif-sur-Yvette, France.

^d Institut des Sciences Moléculaires d'Orsay (ISMO), Université Paris-Saclay, CNRS, 91405, Orsay, France

Table of Content

1. MATERIAL AND METHODS.....	2
1.1. SYNTHESIS OF BODIPY-ANILINE PALMITATE.....	2
1.2. NANOPARTICLE FORMULATION.....	4
1.3. PHOTOPHYSICAL MEASUREMENTS	4
1.4. PHOTOACOUSTIC SPECTRA MEASUREMENTS.....	4
2. RESULTS.....	5
2.1. Z POTENTIAL	5
2.2. TRANSMISSION ELECTRON MICROSCOPY	5
2.3. ABSORPTION COEFFICIENT PER MOLE OF PARTICLES.....	5
2.4. FLUORESCENCE, ABSORPTION AND PHOTOACOUSTIC SPECTRA.....	6
2.5. SPECTRA MODELLING.....	7
2.6. PHOTOACOUSTIC SPECTRA AT DIFFERENT TEMPERATURES.....	12
2.7. PHOTOSTABILITY UNDER LASER EXCITATION.....	13
2.8. PHOTOACOUSTIC SIGNAL VARIABILITY WITH THE LASER FLUENCE.....	13
2.9. TRANSIENT ABSORPTION SIGNAL	13

1. Material and methods

1.1. Synthesis of BODIPY-aniline palmitate.

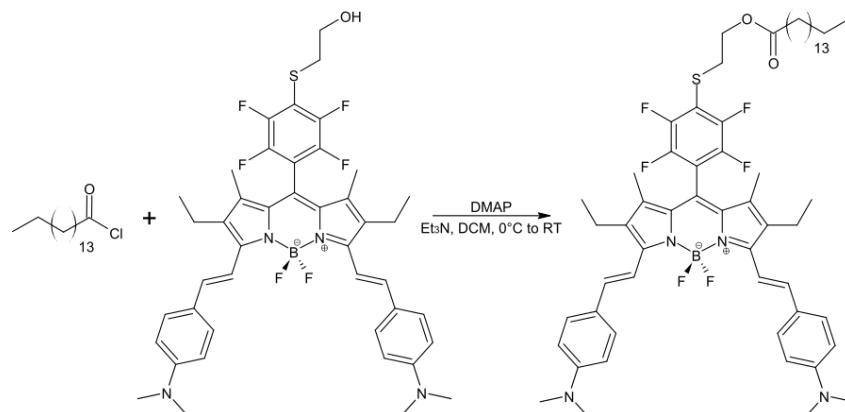


Fig. S1: Reaction scheme (esterification) to form BODIPY-aniline-palmitate (BY-aniline-Palm)

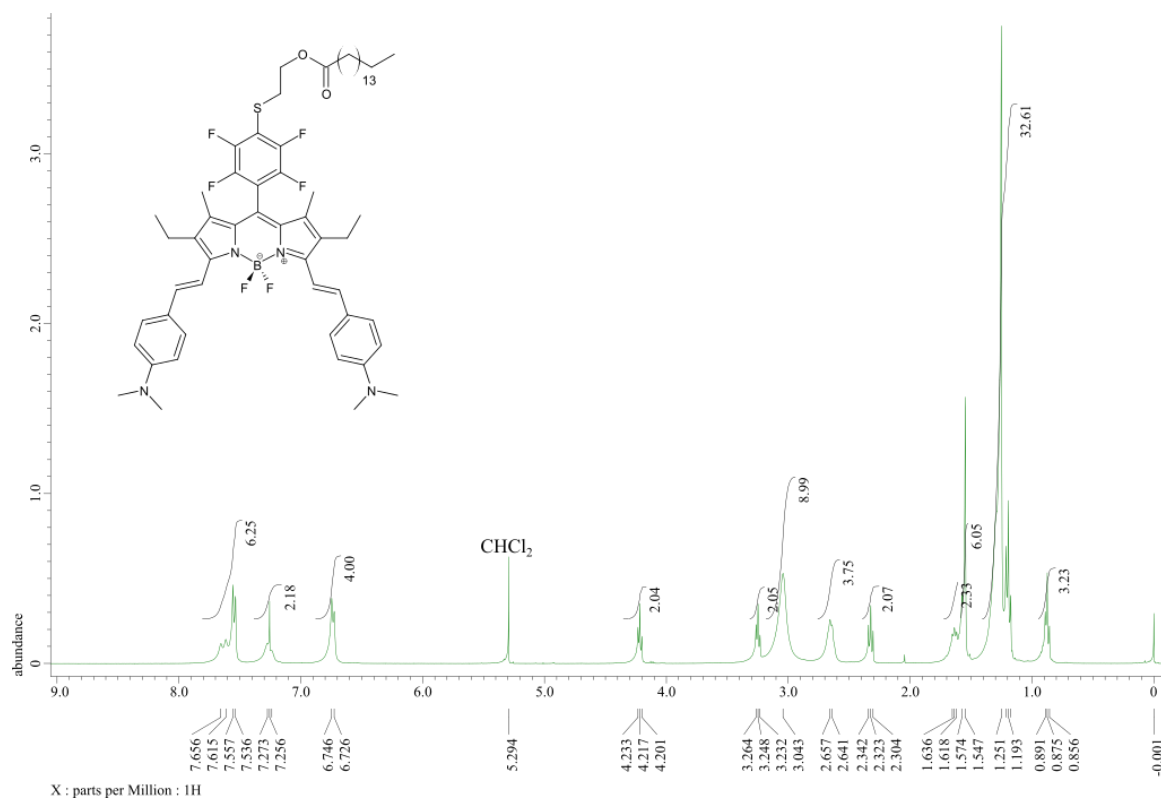


Fig. S2: ¹H NMR of BY-aniline-Palm

1.2. Nanoparticle Formulation.

Table S1 – BY-aniline-Palm (or BY-aniline -PLA) concentrations in SLN and PLA NPs with dilution factor to reach the same concentration.

	SLN-1%	SLN-2%	SLN-6%	SLN-12%	SLN-25%	SLN-50%	SLN-75%	SLN-100%	BY-aniline-PLA-47%
BY-aniline-Palm (or BY-aniline -PLA) concentration (mg.mL⁻¹)	0.0810	0.161	0.472	0.910	1.76	3.10	4.15	5.00	2.35
BY-aniline concentration (mM)	$7.87 \cdot 10^{-2}$	$1.57 \cdot 10^{-1}$	$4.58 \cdot 10^{-1}$	$8.84 \cdot 10^{-1}$	1.71	3.01	4.04	4.86	$1.57 \cdot 10^{-1}$
Dilution factor (to $1.73 \cdot 10^{-2}$ mM)	4.5	9.0	26	51	100	169	230	280	9.0

1.3. Photophysical Measurements

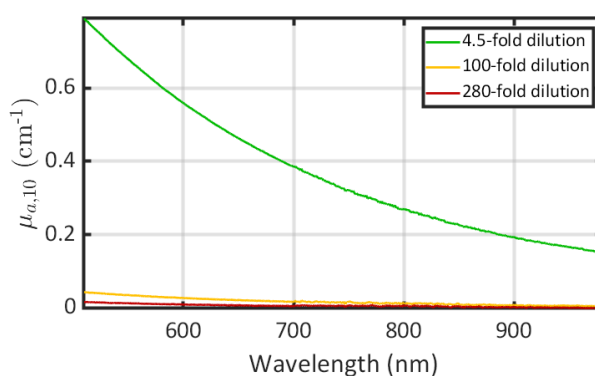


Fig. S5: Unloaded particles (SLN-0%) attenuation spectra used as blank for SLNs. The spectrum was measured for each needed dilution factor. Here 3 representative dilutions corresponding to SLN-1%, SLN-25% and SLN-100%, respectively.

1.4. Photoacoustic Spectra Measurements.

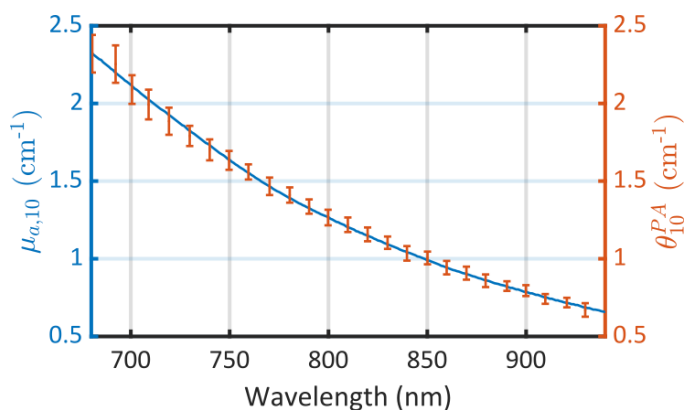


Fig. S6: Absorption and PA spectra of the solution of nigrosin with a PGE equal to 1.

2. Results

2.1. ζ Potential

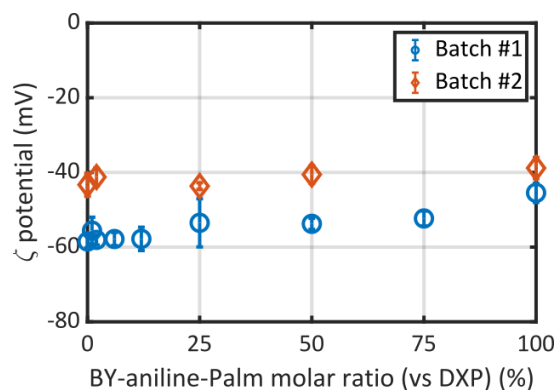


Fig. S7: Evolution of the Zeta potential as a function of the BY-aniline-Palm molar ratio (vs DXP). Markers are blue circle for Batch #1 and orange diamonds for Batch #2. Measurements were done with 20-fold dilution in NaCl 1 mM and error bars are standard deviations on 3 measurements.

2.2. Transmission Electron Microscopy

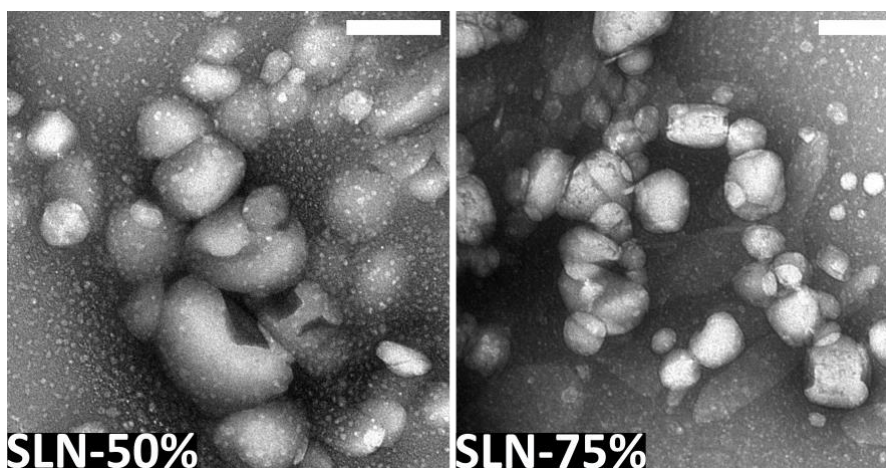


Fig. S8: TEM images of SLN-50% and SLN-75%, obtained with negative staining (uranyl acetate 2% w/w) and acquired with a JEOL JEM-1400 microscope at an acceleration voltage of 120 kV. Magnifications for SLN-50% and SLN-75% are 15,000 and 20,000, respectively. White scale bars on the top right corner represent 200 nm.

2.3. Absorption coefficient per mole of particles

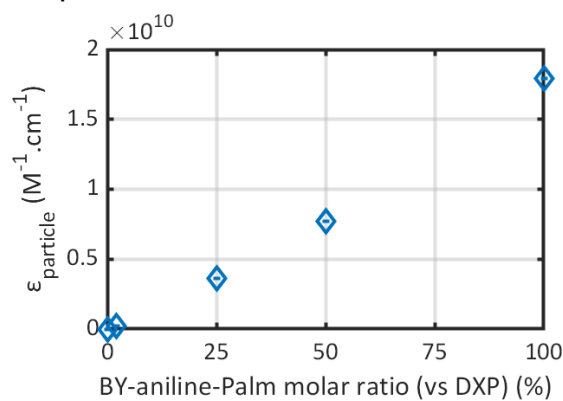


Fig. S9: Evolution of the absorption coefficient per mole of particles evaluated at the maximum absorption wavelength ($\epsilon_{\text{particle}}$) as a function of the BY-aniline-Palm molar ratio (vs DXP) and determined on Batch #2.

2.4. Fluorescence, absorption and photoacoustic spectra

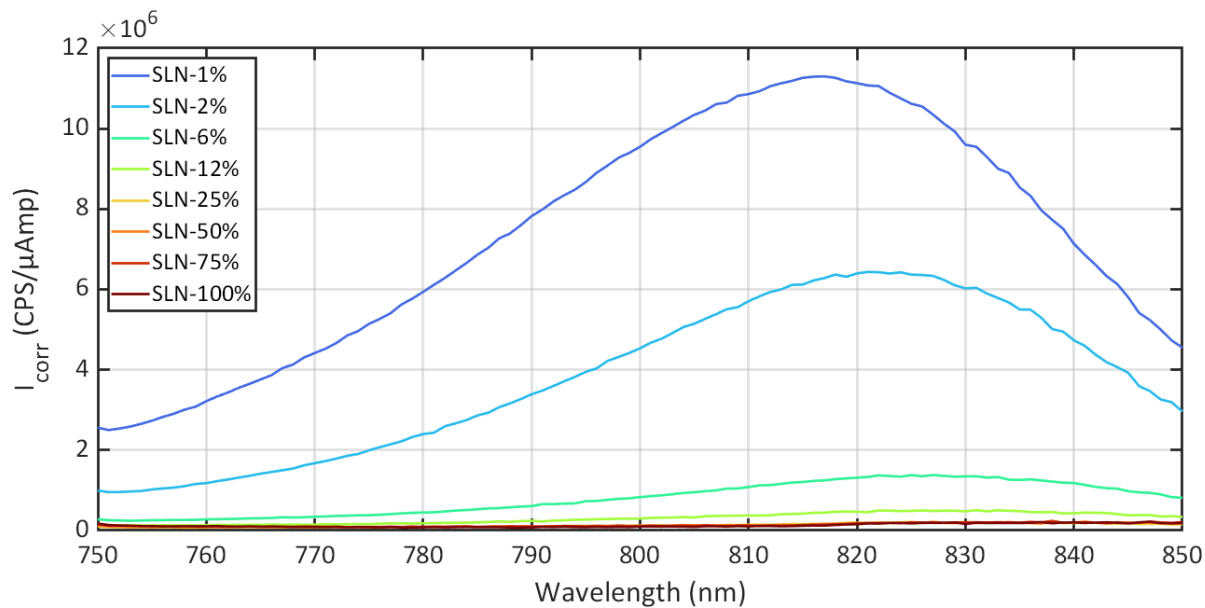


Fig. S10: Fluorescence spectrum ($\lambda_{ex} = 730$ nm, slits width 10 nm and $A < 0.1$) of each type of SLN. The amplitude was corrected by the absorbance at 730 nm.

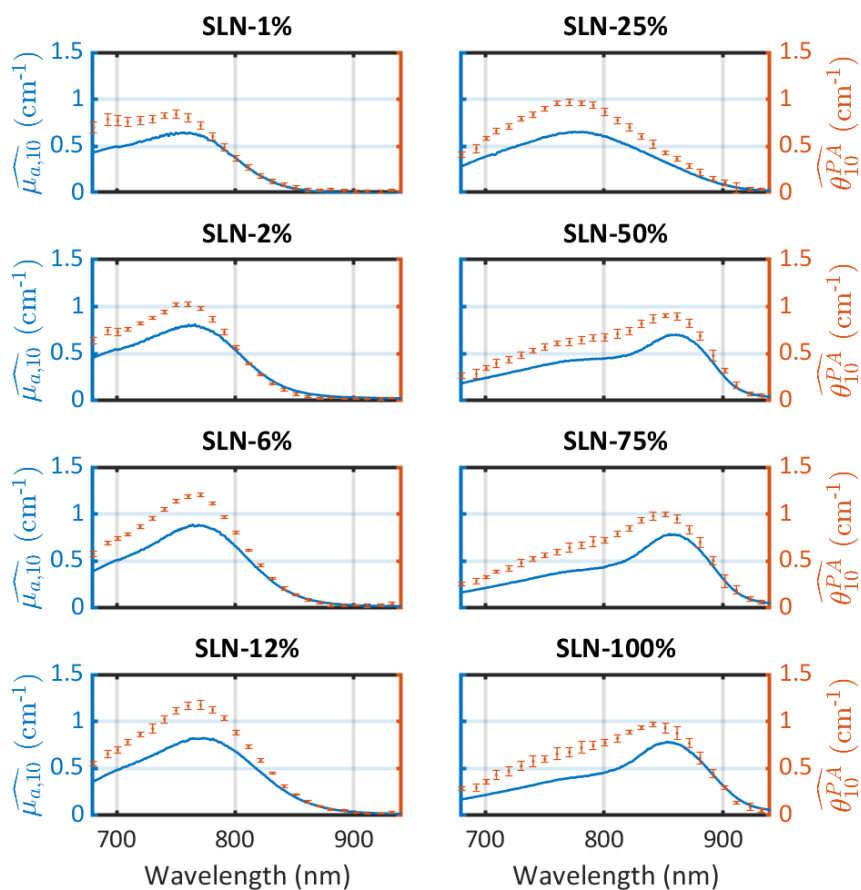


Fig. S11: Superposition of the absorption (blue) and PA (orange) spectra for each SLN (Batch #1).

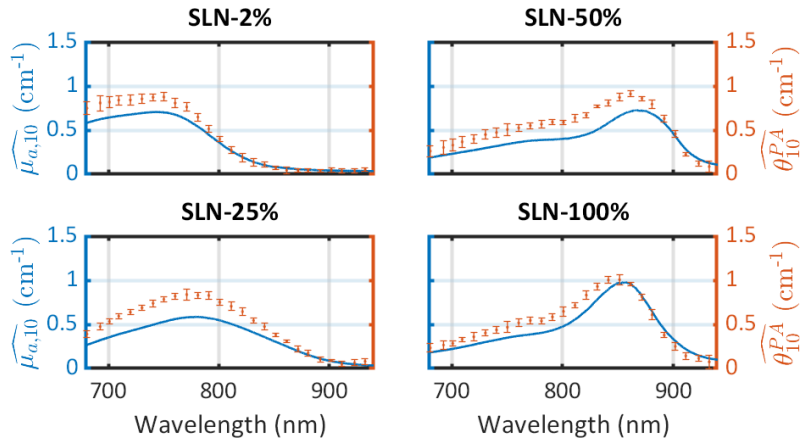


Fig. S12: Superposition of the absorption (blue) and PA (orange) spectra for each SLN (Batch #2).

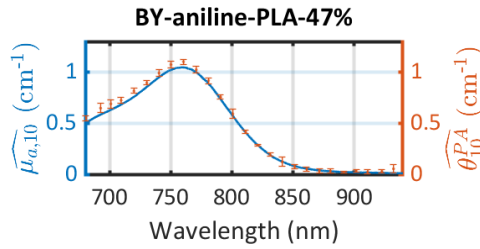


Fig. S13: Superimposition of the absorption (blue) and PA (orange) spectra for BY-aniline-PLA-47% NPs.

2.5. Spectra modelling

Table S2 – Parameters determined for the Gaussian decomposition of the absorption spectra and the PA spectra of Batch #1. a_i (cm^{-1}) is the amplitude of the gaussian curve, λ_i (nm) is the central wavelength and ω_i (nm) is proportional to the full width half maximum ($FWHM_i = 2\sqrt{2 \ln 2} \cdot \omega_i$). Band photoacoustic efficiencies (BPAE) were defined as in the Material and Methods section as the ratio between the PA band area and the corresponding absorption band area. As the widths ω_i are set equal for PA and absorption, BPAE corresponds to an amplitude ratio.

		SLN-1%	SLN-2%	SLN-6%	SLN-12%	SLN-25%	SLN-50%	SLN-75%	SLN-100%	
Absorption	Gaussian #1	a_1					0.51	0.56	0.53	
		λ_1					865	864	863	
		ω_1					26.5	26.5	26.5	
	Gaussian #2	a_2	0.57	0.73	0.85	0.80	0.63	0.42	0.40	0.43
		λ_2	765	769	770	773	783	789	798	799
		ω_2	37.4	39.8	41.8	46.5	59.5	58.6	59.5	59.5
	Gaussian #3	a_3	0.4	0.4	0.31	0.26	0.15	0.11	0.11	0.12
		λ_3	685	685	685	685	685	685	685	685
		ω_3	41.0	41.6	38.0	38.0	45.2	49.4	52.8	46.2
PA	Gaussian #1	a'_1					0.60	0.59	0.51	
		λ'_1					863	860	858	
		ω_1					26.5	26.5	26.5	
	Gaussian #2	a'_2	0.66	0.89	1.13	1.12	0.94	0.65	0.67	0.72
		λ'_2	762	764	767	769	778	791	799	797
		ω_2	37.4	39.8	41.8	46.5	59.5	58.6	59.5	59.5
	Gaussian #3	a'_3	0.64	0.53	0.44	0.35	0.18	0.16	0.17	0.18
		λ'_3	685	685	685	685	685	685	685	685
		ω_3	41.0	41.6	38.0	38.0	45.2	49.4	52.8	46.2
BPAE	Gaussian #1	$\frac{a'_1}{a_1}$					1.18	1.06	0.96	
	Gaussian #2	$\frac{a'_2}{a_2}$	1.16	1.21	1.33	1.41	1.49	1.54	1.67	1.70
	Gaussian #3	$\frac{a'_3}{a_3}$	1.61	1.32	1.41	1.37	1.19	1.41	1.52	1.55

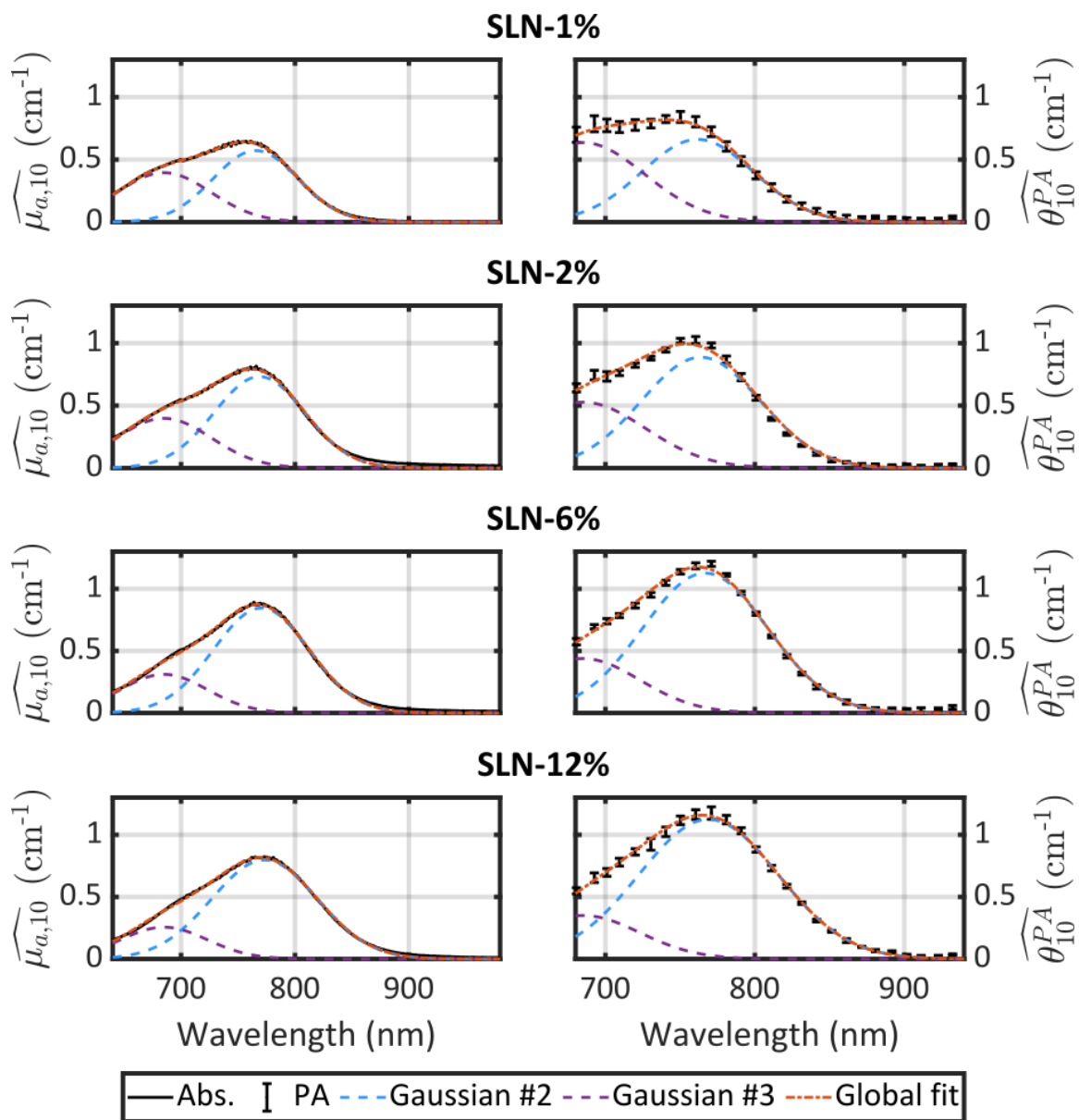


Fig. S14: Gaussian decomposition of absorption and PA spectra for SLN of Batch #1 with BY-aniline-Palm percentage below 25% (excluded).

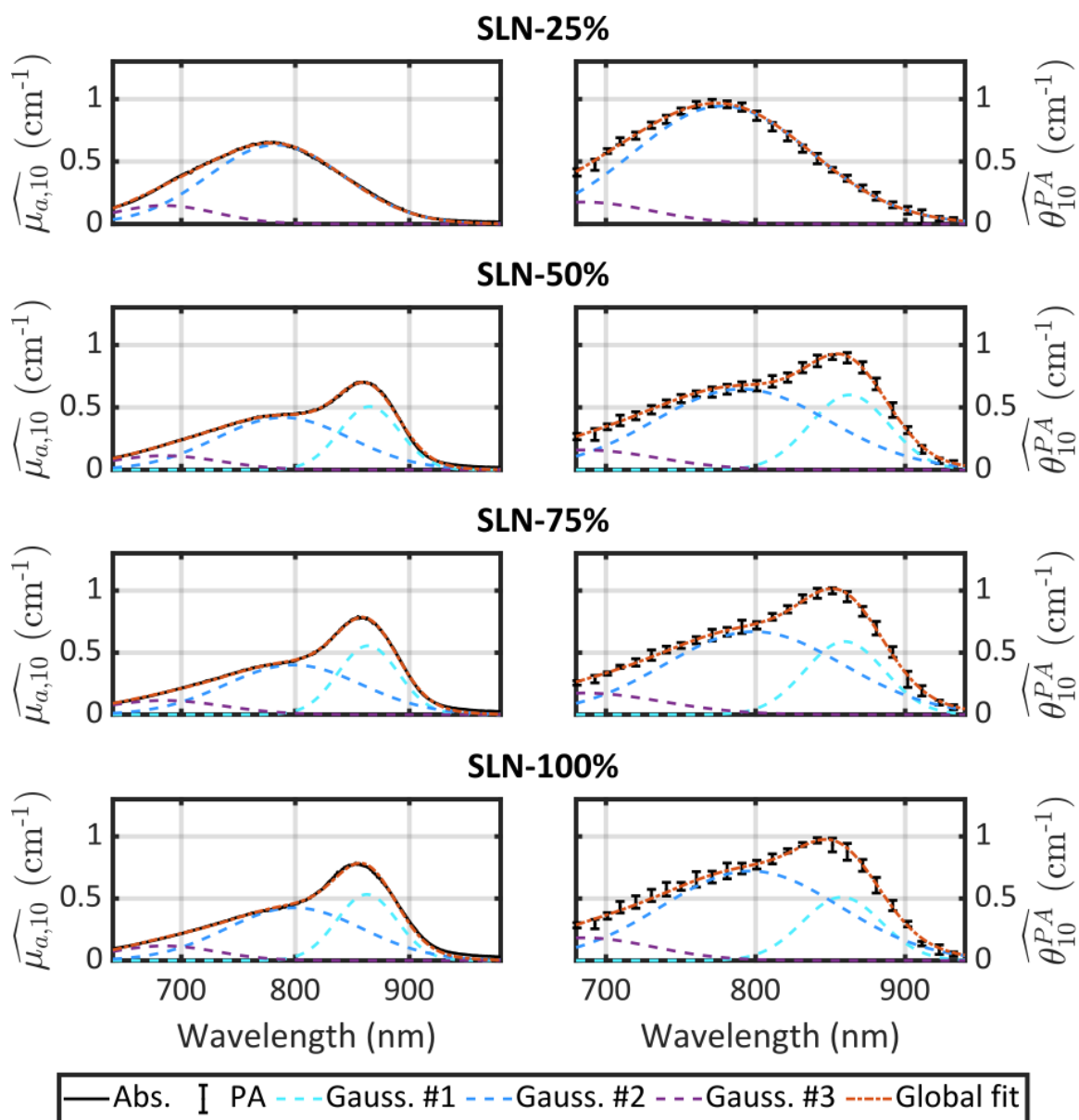


Fig. S15: Gaussian decomposition of absorption and PA spectra for SLN of Batch #1 with BY-aniline-Palm percentage above 25% (included)

Table S3 – Parameters determined for the Gaussian decomposition of the absorption spectra and the PA spectra of Batch #2 and BY-aniline-PLA-47%. a_i (cm^{-1}) is the amplitude of the gaussian curve, λ_i (nm) is the central wavelength and ω_i (nm) is proportional to the full width half maximum ($FWHM_i = 2\sqrt{2 \ln 2} \cdot \omega_i$). BPAE was defined as in Table S2.

		SLN-2%	SLN-25%	SLN-50%	SLN-100%	BY-aniline-PLA-47%	
Absorption	Gaussian #1	a_1		0.56	0.71		
		λ_1		875	859		
		ω_1		26.5	26.5		
	Gaussian #2	a_2	0.47	0.56	0.40	0.41	0.96
		λ_2	763	784	799	799	764
		ω_2	43.2	59.5	59.5	59.5	37.3
	Gaussian #3	a_3	0.50	0.14	0.14	0.13	0.43
		λ_3	685	685	685	685	685
		ω_3	54.0	45.3	46.5	46.2	40.3
PA	Gaussian #1	a'_1		0.61	0.66		
		λ'_1		870	854		
		ω_1		26.5	26.5		
	Gaussian #2	a'_2	0.56	0.81	0.59	0.55	1.00
		λ'_2	759	779	800	797	764
		ω_2	43.2	59.5	59.5	59.5	37.3
	Gaussian #3	a'_3	0.63	0.20	0.21	0.15	0.47
		λ'_3	685	685	685	685	685
		ω_3	54.0	45.3	46.5	46.2	40.3
BPAE	Gaussian #1	$\frac{a'_1}{a_1}$		1.09	0.93		
	Gaussian #2	$\frac{a'_2}{a_2}$	1.19	1.44	1.46	1.32	1.04
	Gaussian #3	$\frac{a'_3}{a_3}$	1.26	1.38	1.45	1.16	1.11

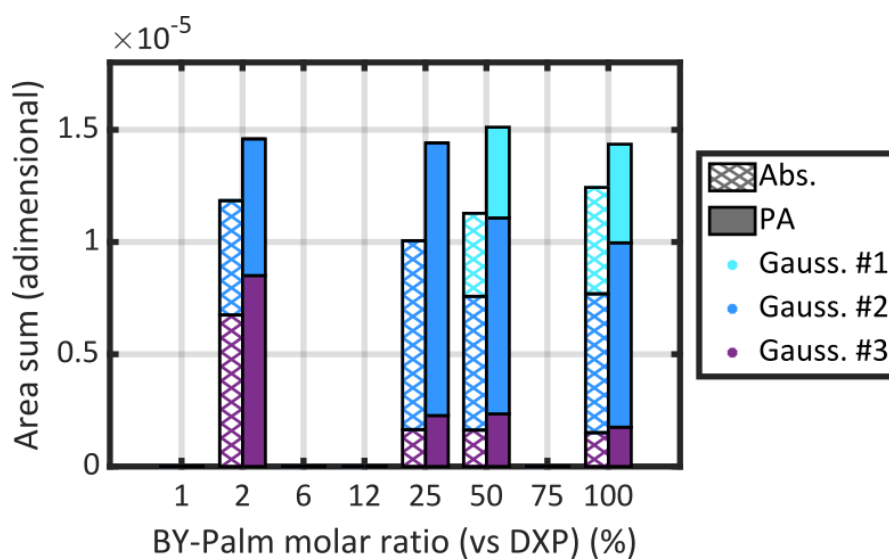


Fig. S16: Contribution of each Gaussian function (area) in the total spectrum area for each SLN of Batch #2. Absorption spectra are on the left-hand side in hatched bars while PA spectra are on the right-hand side in coloured bars.

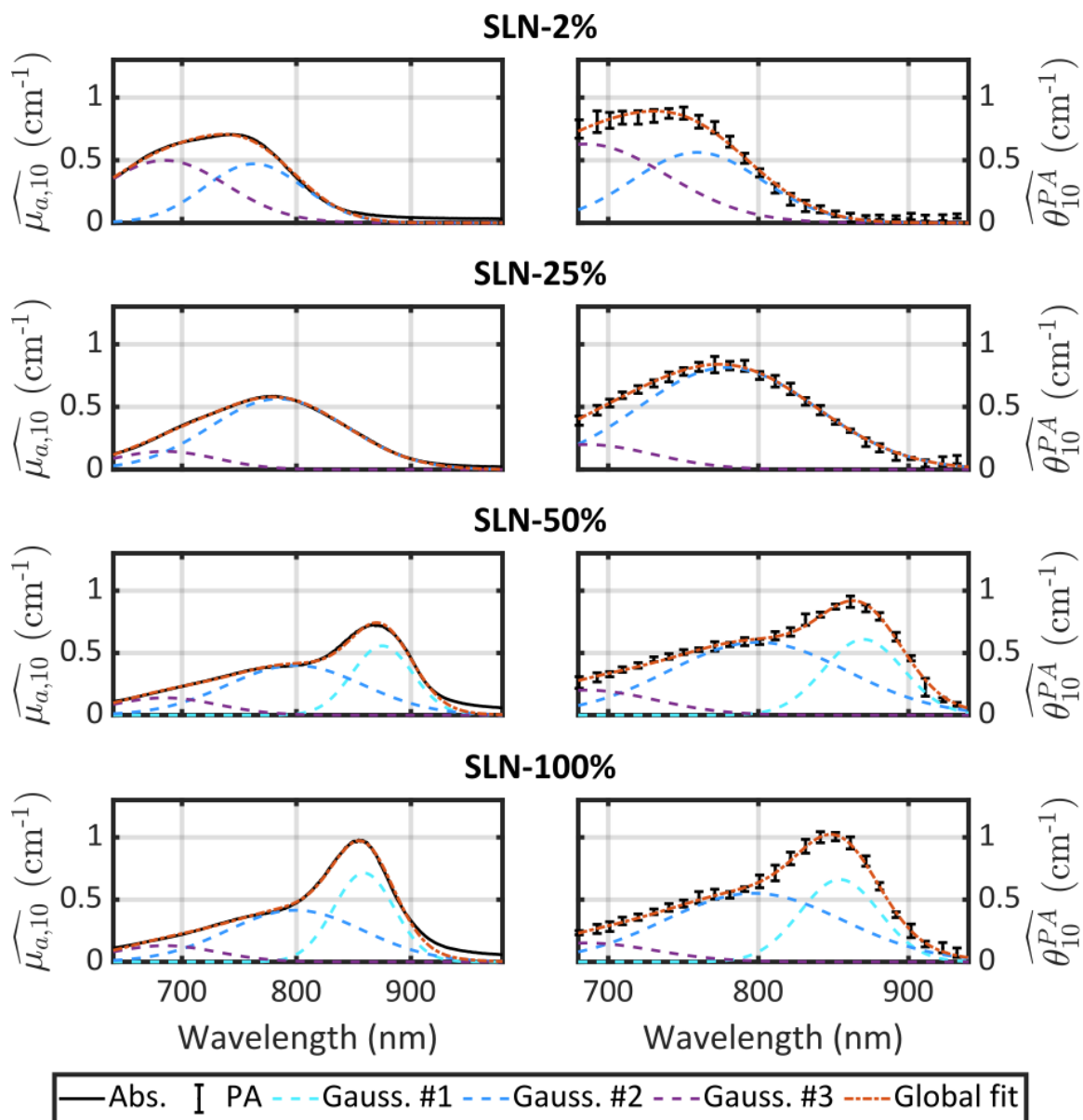


Fig. S17: Gaussian decomposition of absorption and PA spectra for SLNs of Batch #2.

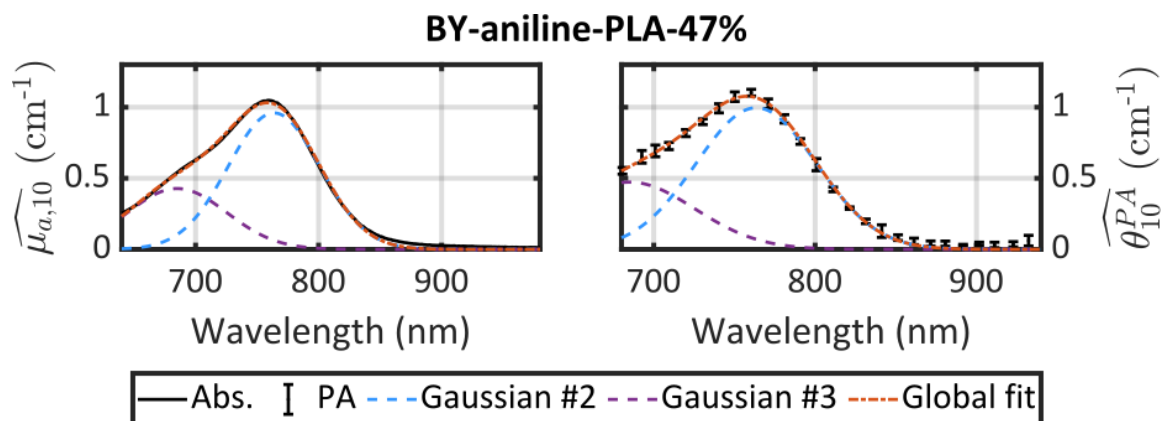


Fig. S18: Gaussian decomposition of absorption and PA spectra for BY-aniline-PLA-47%

2.6. Photoacoustic spectra at different temperatures

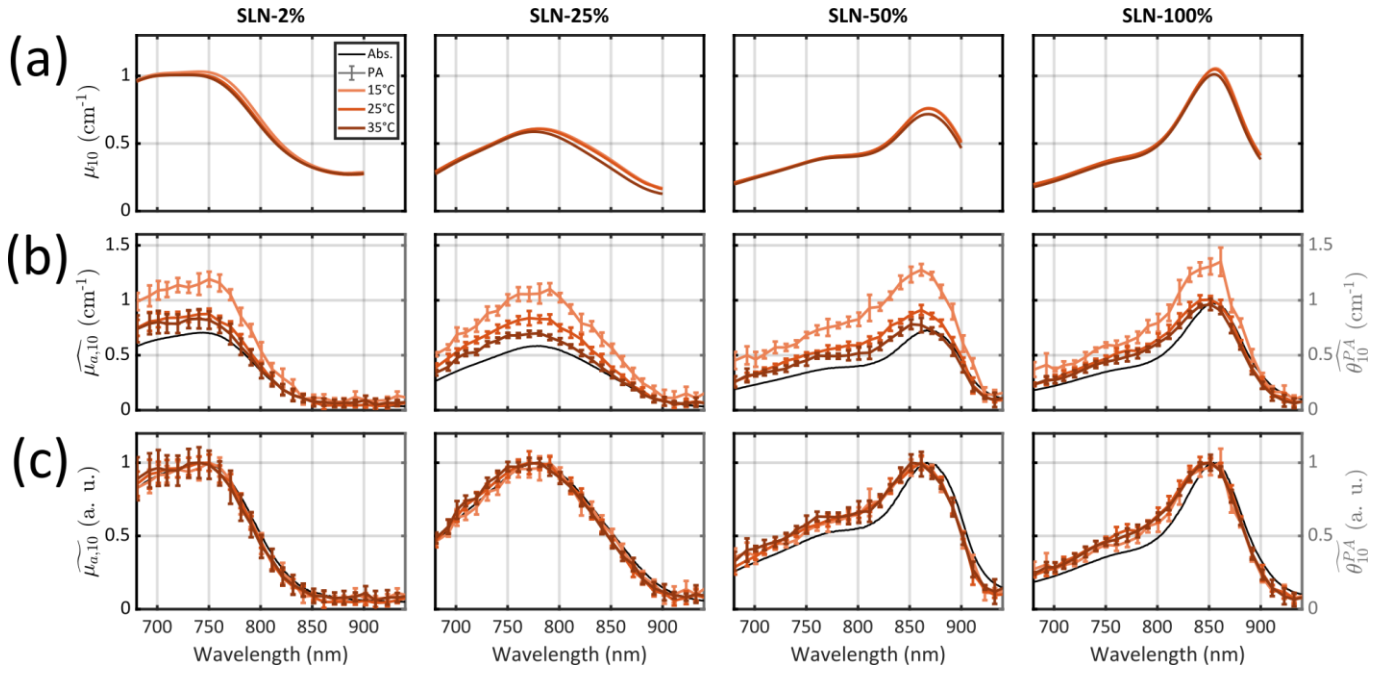


Fig. S19: (a) Absorbance spectra measured at three temperatures (15°C, 25°C and 35°C) of SLNs from batch #2. Measurements at different temperatures are color-coded with shades of orange. The scattering was not corrected. (b) PA spectra at three temperatures (15°C, 25°C and 35°C) of SLNs. The absorption spectra (corrected for scattering) are displayed with a black solid line. (c) Normalized absorption and PA spectra at three temperatures (15°C, 25°C and 35°C) of SLNs. Each spectrum is normalized by the spectrum maximum. The colour code is the same in (a) (b) and (c).

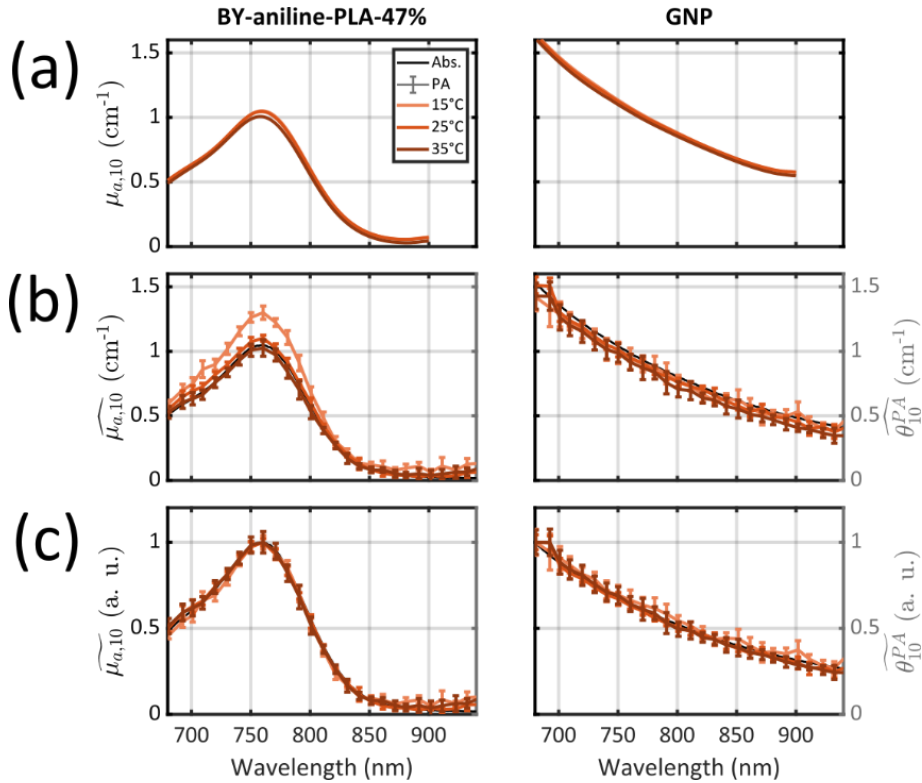


Fig. S20: (a) Absorbance spectra measured at three temperatures (15°C, 25°C and 35°C) of PLA NPs (left) and GNPs (right). Measurements at different temperatures are color-coded with shades of orange. The scattering was not corrected. (b) PA spectra at three temperatures (15°C, 25°C and 35°C) of PLA NPs (left) and GNPs (right). The absorption spectra (corrected for scattering) are displayed with a black solid line. (c) Normalized absorption and PA spectra at three temperatures (15°C, 25°C and 35°C) of PLA NPs (left) and GNPs (right). Each spectrum is normalized by the spectrum maximum. The colour code is the same in (a) (b) and (c).

Table S4 – Global photoacoustic efficiencies (GPAE) for Batch #1 were defined in the Material and Method section as the ratio between the integral of the PA spectrum and the integral of the equivalent absorption spectrum on the interval [680 nm, 920 nm]. It corresponds as the weighted mean PGE over the whole spectrum.

	SLN-1%	SLN-2%	SLN-6%	SLN-12%	SLN-25%	SLN-50%	SLN-75%	SLN-100%
GPAE 25°C	1.31	1.21	1.32	1.39	1.43	1.4	1.44	1.43

Table S5 – Global photoacoustic efficiencies (GPAE) for Batch #2, GNP and BY-aniline-PLA-47% were computed as defined in Table S4.

	SLN-2%	SLN-25%	SLN-50%	SLN-100%	BY-aniline-PLA-47%	GNP
GPAE 15°C	1.65	1.84	1.88	1.47	1.24	0.96
GPAE 25°C	1.2	1.4	1.34	1.15	1.05	0.97
GPAE 35°C	1.16	1.19	1.17	1.08	0.98	0.92

2.7. Photostability under laser excitation

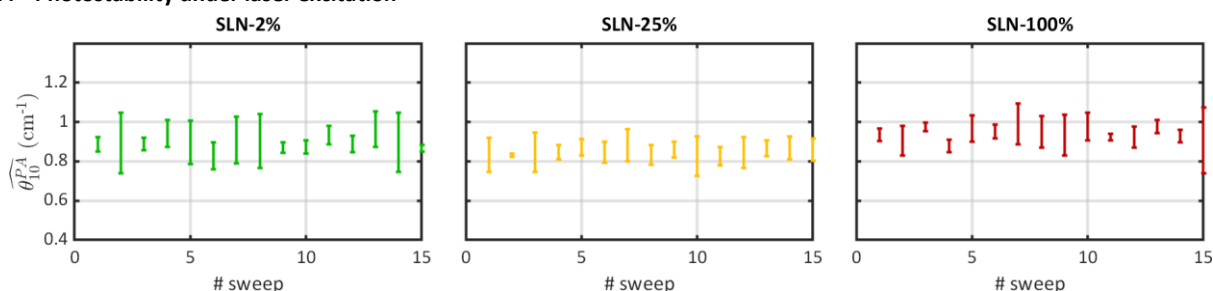


Fig. S21: Photoacoustic coefficients as a function of the number of the sweeps. The PA coefficients are measured at the maximum absorption wavelength, namely : 750 nm for SLN-2% (green), 780 nm for SLN-25% (yellow) and 960 nm for SLN-100% (red), respectively. For each sweep, the acquisition was performed simultaneously on four tubes and the displayed results corresponds to the median (with the MAD as error bar) over the 4 tubes.

2.8. Photoacoustic signal variability with the laser fluence

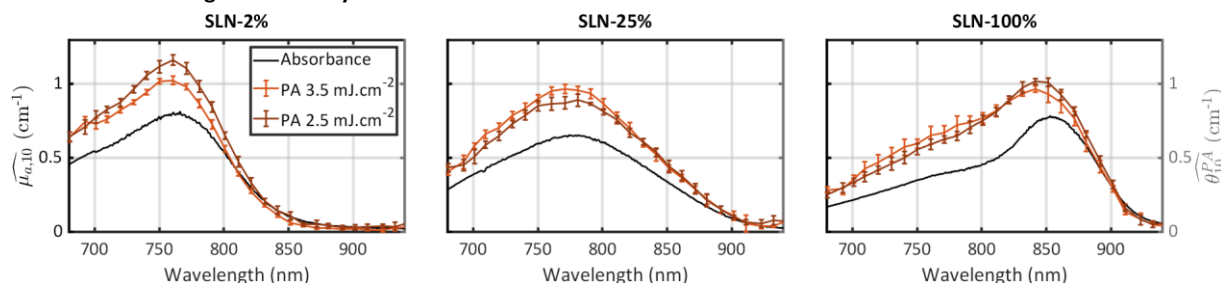


Fig. S22: Superimposition of the absorption and PA spectra for three formulations (SLN-2%, SLN-25% and SLN-100%). Two different laser fluences are used: 3.5 mJ.cm⁻² (orange) and 2.5 mJ.cm⁻² (brown). The mean variation between the spectra at the two fluences is below 10%.

2.9. Transient absorption signal

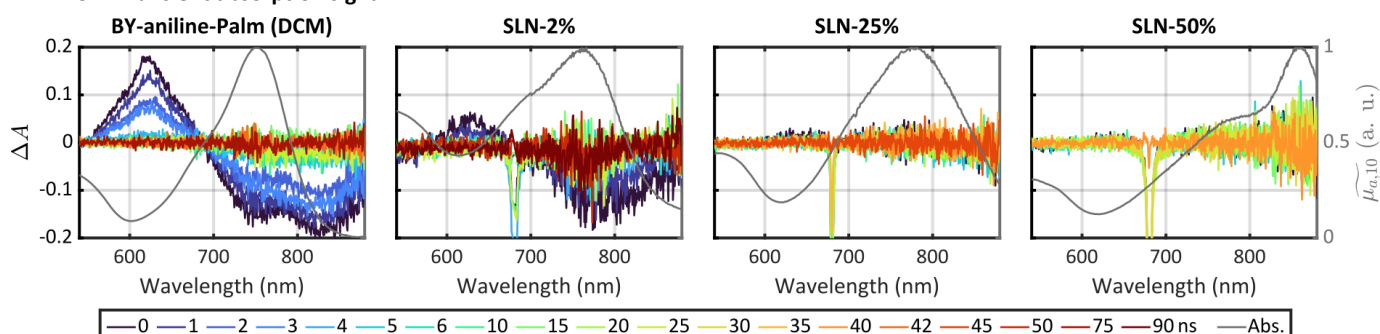


Fig. S23: Transient absorption spectra of BY-aniline-Palm in DCM, SLN-2%, SLN-25% and SLN-50% for different time delays (in ns and color-coded) between pump (at 680 nm) and probe. Normalized equivalent absorption spectra are displayed in grey.